Polymer 49 (2008) 3524–3532

Contents lists available at ScienceDirect

Polymer

journal homepage: www.elsevier.com/locate/polymer

Destruction and formation of a carbon nanotube network in polymer melts: Rheology and conductivity spectroscopy

Ingo Alig [a,*], Tetyana Skipa [a], Dirk Lellinger [a], Petra Pötschke [b]

[a] Deutsches Kunststoff-Institut, Schlossgartenstraße 6, D-64289 Darmstadt, Germany
[b] Leibniz-Institut für Polymerforschung Dresden e.V. Hohe Straße 6, D-01069 Dresden, Germany

ARTICLE INFO

Article history:
Received 5 February 2008
Received in revised form 15 May 2008
Accepted 19 May 2008
Available online 3 June 2008

Keywords:
Carbon nanotube network
Conductivity recovery
Polymer melt

ABSTRACT

Destruction and formation of the carbon nanotube network in polymer melts have been investigated by a combination of conductivity spectroscopy and dynamic-mechanical analysis for polycarbonate (PC) containing multiwalled carbon nanotubes. The combined setup allows simultaneous time-resolved measurements of electrical conductivity, dielectric permittivity and dynamic shear modulus. Furthermore, well-defined shear deformations can be applied to the samples. After annealing the samples well above glass transition short shear deformations were applied to the melt. These deformations lead to a decrease of the conductivity by about 6 orders of magnitude and of the real part of the shear modulus (G') by a factor of 20. In the rest time after the shear deformation a complete recovery of the conductivity and G' modulus was observed. The changes in conductivity and G' were assigned to destruction and reformation of agglomerates, which are assumed to be conductive spherical objects containing loosely packed nanotubes. For a quantitative description of the time dependent electrical conductivity a simple model combining cluster aggregation and electrical percolation is applied.

1. Introduction

It is known over decades that filling of electrically insulating polymers even with small amounts (only few percent) of conducting particles results in an increase of the electrical conductivity of composites by orders of magnitude and can lead to a mechanical reinforcement [1–3]. Carbon nanotubes (CNTs) as fillers were found to improve electrical and mechanical properties of polymer matrices similar to carbon black (CB) particles with the advantage that for building up the conductive percolation network much lower weight content of CNT is needed [4–11]. This is related to the high aspect ratio (ratio between length and diameter) of CNT (about 100–1000) compared to more spherical CB particles. This geometrical advantage as well as the huge nanotube stiffness and their high thermal and electrical conductivities makes CNT-based materials attractive for new applications. Therefore, carbon nanotube–polymer composites belong to a fast-developing field of material science, which is in close contact with the industrial needs.

The enhancements of thermal, electrical and mechanical characteristics of nanotube–polymer composites are attributed to the formation of a network of interconnected filler particles which can either conduct heat and electrical current or relax mechanical stress without a large matrix deformation [1–3]. Studies on thermoplastic polymers, melt compounded with both singlewalled (SWNT) and multiwalled carbon nanotubes (MWNTs), show electrical percolation at concentrations ranging from 0.05 vol% towards 5 wt% [4–15]. The percolation concentrations were found to depend strongly on the nanotube length, diameter, degree of purification, bundling, type of matrix polymer and on the processing of the composite (e.g. temperature and mixing conditions, for example, see Refs. [12,14,16]). All these factors result in a wide variation in electrical conductivity and other material properties of the finished plastic products and appear to be one of the major restraints for a broad market acceptance of this new class of polymer nanocomposites.

Some years ago, our group reported on the influence of the extrusion conditions on the electrical conductivity of polycarbonate–MWNT mixtures using conductivity spectroscopy [11]. The conductivity measurements have shown the influence of screw speed and mixing time on the dispersion of the nanotubes. We assumed that even small geometrical changes in the local contact regions between the nanotubes – which are usually separated by polymer chains – can lead to considerable changes in the contact resistance and contact capacity. More recently it was shown by time-resolved conductivity measurements during isothermal annealing of pressed plates (polypropylene containing 2 wt% MWNT) that the thermal treatment above the melting temperature leads to an increase of the conductivity by about 10 orders of

* Corresponding author. Tel.: +49 6151 16 2404; fax: +49 6151 29 2855.
E-mail address: ialig@dki.tu-darmstadt.de (I. Alig).

0032-3861/$ – see front matter © 2008 Elsevier Ltd. All rights reserved.
doi:10.1016/j.polymer.2008.05.037

magnitude in 10 h [16]. This is an indication of the formation of a conductive network in the melt during annealing. A similar conductivity recovery was observed in a slit die for polypropylene containing 2 wt% MWNT which was flanged to the outlet of an extruder, after stopping extrusion for some time [17]. For a similar in-line setup, we found such conductivity recovery as well for polycarbonate and polyamide at different melt temperatures [18]. Zhang et al. [19] found a similar conductivity recovery during melt annealing of polyethylene/poly(methyl)methacrylate blends containing carbon black and carbon fibres in one of the phases. Using a combined rheological-dielectric setup the conductivity recovery was detected after a short shear deformation (shear rate $d\gamma/dt = 1\ s^{-1}$ for 10 s) for MWNT in polycarbonate in a well-defined laboratory experiment [20]. The decrease of the electrical conductivity with increasing shear rate was first reported by Kharchenko et al. [21] for polypropylene containing MWNT. Obrzut et al. also observed a shear-induced conductor–insulator transition of CNT in PP melts during shear [22]. These experiments have been performed under steady shear conditions. They also reported on a conductivity recovery after steady state shearing ($d\gamma/dt = 6.3\ s^{-1}$) was stopped. Using polarized light-scattering experiments on a weakly elastic melt, Hobbie et al. [23] showed that the tubes orient along the direction of flow already at low shear stresses, with a transition to vortices' alignment above a critical shear stress. More recently, Hobbie and Fry [24] measured the rheological properties of carbon nanotubes suspended in low-molecular-mass polyisobutylene using a polysuccinimide dispersant over a range of nanotube volume fractions. Using controlled strain rate and controlled stress measurements of yielding in shear flow, they proposed a universal scaling of both the linear viscoelastic and steady-shear viscometric responses.

The aim of this paper is to study the kinetics of destruction and reformation of a conductive CNT network in a polymer melt by simultaneous time resolved measurements of electrical conductivity and dynamic shear modulus during thermal annealing and after well-defined (short) shear deformations. For a quantitative description of the conductivity recovery after shear deformation a combined model of cluster aggregation and electrical percolation was developed [20]. For the agglomeration of CNT a second order kinetics was used, which was proposed for agglomeration of filler particles in a polymer matrix by Heinrich et al. [25]. The idea of conductive filler agglomeration was reported before by Schüler and co-workers [26,27] for reactive epoxy mixtures containing carbon black.

Here we performed studies on polycarbonate filled with 0.6 vol% of MWNT, which is close to the concentration of electrical percolation. We expect that besides its practical interest for polymer–CNT composites, this study may contribute to the understanding of agglomeration of fillers in polymer melts in general.

2. Experimental

2.1. Sample characterization and preparation prehistory

Polycarbonate composites filled with 0.6 vol% (corresponding to 0.875 wt%) of multiwalled carbon nanotubes (MWNTs) were prepared by melt dilution of a masterbatch containing 15 wt% MWNT (Hyperion Catalysis International, Cambridge, MA) using a DACA Microcompounder (DACA Instruments, Goleta, USA) as described in Ref. [13]. The extruded strands were compression molded into sheets with a thickness of about 600 μm at 265 °C for about 1 min at 50 kN [20]. The nanotubes were originally produced by chemical vapor deposition and typically consist of 8–15 graphite layers, with diameters of 10–15 nm and a length distribution between 1 and 10 μm. A transmission electron microscopic image of a PC–MWNT composite similar to that in our investigations is seen in Fig. 1a (reproduced from Ref. [20]). This image shows that the nanotubes in the samples before annealing are quite well-dispersed and have a curved shape. However, some nanotube orientation parallel to the surface induced by the squeeze flow and some minimal aggregation as seen in the lower right area cannot be excluded completely. More detailed studies of agglomeration have been performed recently on pressed plates of PC–MWNT composites [28]. Although the nanotubes are well-dispersed and their volume concentration is above the theoretical percolation threshold [29] for the given aspect ratio, the DC conductivity for this sample at room temperature is below 10^{-16} S/cm, which is close to the conductivity of the polymer matrix. Pressing the material at higher temperature ($T = 300$ °C) with otherwise same pressing conditions results in considerable nanotube agglomeration (see Fig. 1b, reproduced from Ref. [20]). Surprisingly, the electrical conductivity of this sample is by 12 orders of magnitude higher (5×10^{-4} S/cm) than that of the sample pressed at lower temperature showing well dispersed nanotubes [20]. It could be assumed that the considerably lower viscosity of the polymer matrix at 300 °C leads to a faster diffusion of the nanotubes and accelerates their agglomeration. Therefore, the formation of conductive agglomerates (Fig. 1c and explanation in 3.3.) is considered to be a key process for understanding the dependence of electrical conductivity on thermal and mechanical prehistory. It has to be stated that in a two-dimensional (2D) cut of a 3D structure close to percolation it is not possible to see through going pathways formed by nanotubes (or agglomerates) directly in the TEM. So it is not surprising that only separated agglomerates or groups of agglomerates can be seen in Fig. 1.

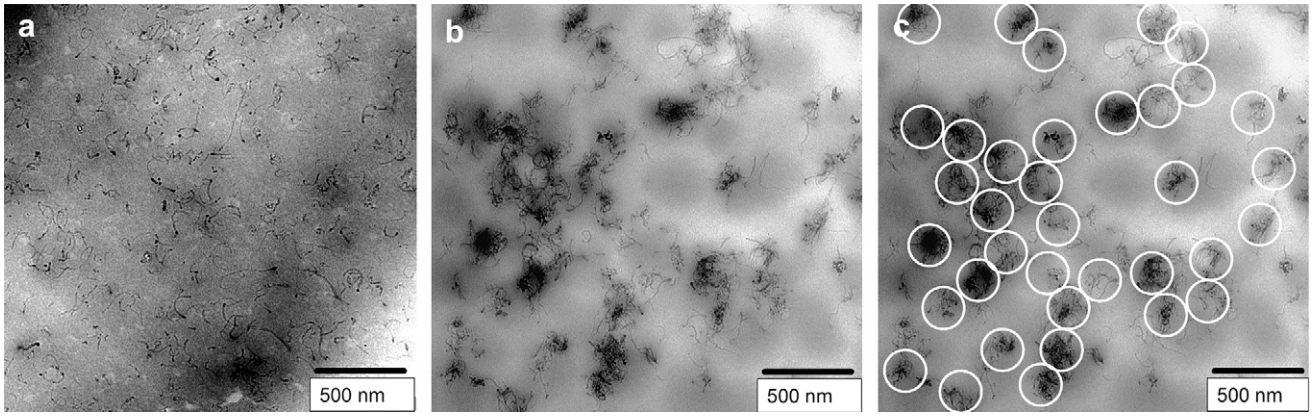

Fig. 1. Transmission electron micrographs from PC–MWNT plates with 0.6 vol% MWNT: (a) non-conductive state ($\sigma_{DC} < 10^{-16}$ S/cm) with well-dispersed nanotubes, pressed at 265 °C and (b,c) conductive state ($\sigma_{DC} = 5 \times 10^{-4}$ S/cm) with nanotube agglomerates pressed at 300 °C.

2.2. Combined rheological and dielectric setup

The combined rheological and dielectric measurements were performed in a rheometer (ARES, Rheometrics Scientific). Both rheometer plates (plate–plate geometry) have been replaced by ring electrodes connected to a frequency response analyser Solartron SI 1260 for the dielectric measurements. In Fig. 2 the ring-shaped PC–MWNT sample between the ring electrodes, with an inner diameter of 18 mm and an outer diameter of 25 mm, and the experimental set-up are schematically given. For the dielectric/rheological measurements, rings with the dimensions of the electrodes were cut from the pressed plates (thickness of 0.6 mm) of the PC–MWNT composites. Such particular ring design allows transient shear experiments with almost constant shear rate through the sample volume.

The dielectric measurements were performed in a frequency range between 1 kHz and 1 MHz. A frequency of $f = 1$ kHz was taken to be representative for the DC conductivity (see below). The data were recorded and processed using the WinDETA software available together with the frequency response analyser Solartron SI 1260 from Novocontrol (Germany). The temperature was controlled by hot nitrogen flow in order to prevent oxidation of the composite under heating.

2.3. Electrical and mechanical measurements

In the first step, the as-received samples were annealed for 2 h at 230 °C in order to achieve an almost defined morphology of the conductive network. Two hours have been chosen as the annealing time, since no significant degradation by thermogravimetric analysis was detected. Then transient shear was applied to the molten samples. In order to study the destruction and the recovery process of the conductive filler network, two different shear regimes were applied to the polymer–CNT melts. In the first experiment, a short shear deformation with shear rate of $d\gamma/dt = 1$ rad/s was applied for 10 s ("single shear"). In the second experiment a "double shear" pulse consisting of a short pre-shear of 10 rad/s for 1 s followed by a second shear pulse ($d\gamma/dt = 1$ rad/s for $t = 10$ s) after 6 min was applied to the melt. The double pulse experiment allows a stronger destruction of the conductive CNT network (see below). In the rest time after shear the electrical conductivity and shear modulus of the composite melt were simultaneously measured. In order to get a sufficient time resolution most of the experiments were performed with a fixed frequency of 1 kHz for dielectric measurements and 1 rad/s for dynamic-mechanical measurements. Dielectric and mechanical spectra were acquired with lower time resolution in the frequency ranges 1 kHz to 1 MHz and 0.3–100 rad/s, respectively.

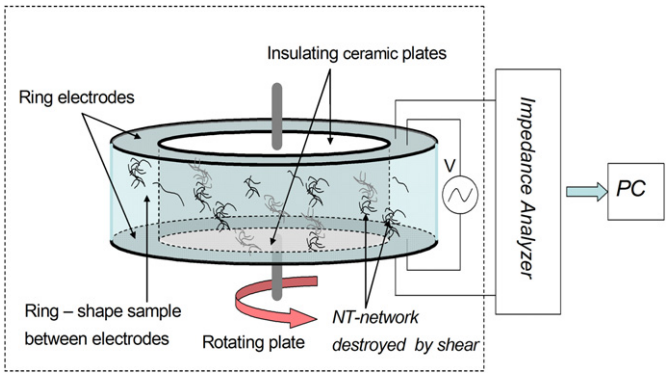

Fig. 2. Schematic representation of the combined setup for simultaneous dielectric and dynamic-mechanical measurements. The ring shaped polymer–nanotube sample is inserted between two ring electrodes.

The dynamic-mechanical measurements were performed in a time-sweep mode with strain amplitude of 1%. Experiments with different strain amplitudes have shown that the influence of an oscillatory shear deformation of 1% on the electrical conductivity is negligible. Other pre-experiments with long-time intervals between the dielectric measurements (with no electric field) indicated that the AC-electrical field with an amplitude of 1 V does not induce any CNT rearrangement either.

3. Results and discussion

3.1. Electrical conductivity

Fig. 3a and b presents the time evolution of the DC conductivities of two identical PC–MWNT samples containing 0.6 vol% MWNT measured for the "single" and "double shear" experiments, respectively. The time region $t < 7200$ s represents isothermal annealing of the fresh samples at 230 °C for 2 h. After annealing the DC conductivities for both samples are similar and reach values of about 10^{-4} S/cm.

At $t \approx 7200$ s the "single shear pulse" or the "double shear pulse" was applied. During this time, in both shear experiments the DC conductivities decrease by about 6 orders of magnitude and almost reach the conductivity of the polymer matrix ($<10^{-10}$ S/cm at $T = 230$ °C). This indicates the destruction of conductive network paths.

The recovery of DC conductivity ($t > 7200$ s, Fig. 3) for both experiments differs substantially. Fig. 4 compares the conductivity recovery for both shear regimes (data from Fig. 3a and b) more in detail. Although both curves have similar shape, the recovery kinetics for the sample with the short pre-shear (double shear experiment) is considerably slower than that for the single shear experiment. After a long recovery period (>5 h) the DC conductivities for both samples reach a level of about 10^{-3} S/cm (not shown), which is restricted by the initial concentration of the nanotubes in the composite. Although the MWNT concentration of the sample is constant, the shape of the DC conductivity curves versus time for both experiments looks similar to a percolation curve for varying contents of conductive filler. This "dynamic" percolation was recently discussed by us in terms of cluster aggregation [20].

The single shear experiment is expected to break down the nanotube network only gradually by rupture of the contacts between the conducting network parts and/or nanotube orientation. For this experiment only a moderate destruction of the nanotube network is assumed. One may speculate that the distance between nanotubes or agglomerates of nanotubes is relatively small and pieces of the conductive network are almost homogeneously distributed in the polymer matrix. Thus the reformation process is relatively fast. However, if the network structure undergoes abrupt and strong shear like in the double shear experiment, CNTs (or pieces of the conducting network) are expected to be separated by longer distances and their spatial distribution becomes less homogeneous. The slower conductivity recovery for the "double shear experiment" can be understood in terms of diffusion controlled reformation of the conducting network parts (e.g. CNT and/or clusters) in a viscous surrounding. Therefore, it is reasonable to assume the same mechanism for the network recovery in both cases with only difference in the recovery speed (or reaction rate [20]) of the agglomeration process. These assumptions are used in Section 3.3 for modelling the conductivity recovery.

The assumption of a "dynamic percolation" is supported by the frequency dependence of the real parts of the complex conductivity σ' and permittivity ε' given in Fig. 5a and b. These spectra were measured with low time resolution after single shear pulse. In order to obtain reasonable spectra no significant change of the

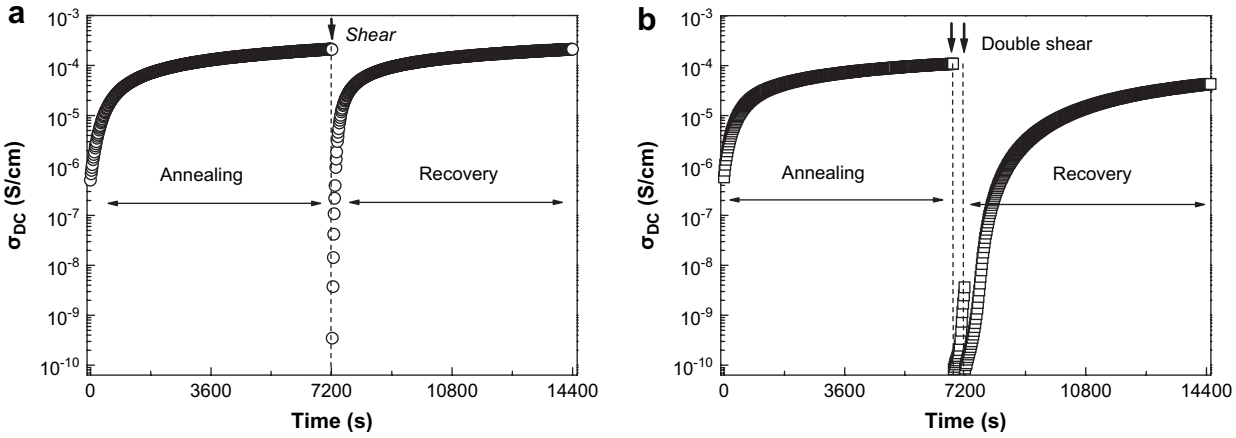

Fig. 3. DC conductivity σ_{DC} during annealing ($T = 230\,^{\circ}C$), transient shear deformation (specific for a and b), and isothermal conductivity recovery after shear at 230 °C: (a) single shear deformation ($t = 10$ s, $d\gamma/dt = 1\ s^{-1}$) and (b) double shear deformation (pre-shear: 10 rad/s for 1 s; second shear: $d\gamma/dt = 1$ rad/s for 10 s).

conductivity (and the underlying percolation structure) should occur in the time interval necessary for the acquisition of one spectrum (minimum 40 s). This is fulfilled only for the spectra recorded at later times after shear and only those spectra are shown.

Two characteristic quantities can be determined from the conductivity spectra measured during the recovery process: (i) the DC conductivity σ_{DC} versus time (see Fig. 3) and (ii) the cross-over frequency $\omega_c = 2\pi f_c$ (see Fig. 5). The latter indicates the transition from the DC plateau to power law behaviour $\sigma'(\omega) \propto \omega^n$ (for details see Ref. [11] and references therein). Assuming that the frequency dependence of the conductivity can be described by charge carrier diffusion on percolation clusters and that the characteristic frequency $\omega_c (= 1/\tau_\xi)$ is inversely proportional to the characteristic time τ_ξ, which is needed for a charge carrier to traverse a cluster of correlation length ξ, ω_c is related to the filler concentration p as follows (see references in Ref. [11]):

$$\omega_c(p) \propto |p - p_c|^{\nu d_w}. \quad (1)$$

The exponent d_w is the effective fractal dimensionality of the random walk ("diffusion exponent") and ν is the exponent of the concentration dependence of the correlation length. The numerical value of the correlation length exponent for 3D percolation was found [30,31] to be $\nu \cong 0.88$. The value of ω_c decreases with concentration below percolation ($p < p_c$) and increases above percolation ($p > p_c$). This can be used for the detection of the percolation threshold p_c. For the analysis of the experimental spectra during conductivity recovery after shear, at each moment a different structure of the conducting network – which is represented by a certain conductivity spectrum – has to be assumed. If one now replaces the CNT content in the percolation theory by the actual content of conducting agglomerates contributing to the electrical percolation path ($p \equiv p_A$), the volume fraction of conducting agglomerates $p_A(t)$ becomes a function of time. The agglomerates can be assumed to evolve from a cluster aggregation process [20]. In such a system, the evolution of the cross-over frequency with time $\omega_c(t)$ can be used as an indicator for the dynamic percolation transition.

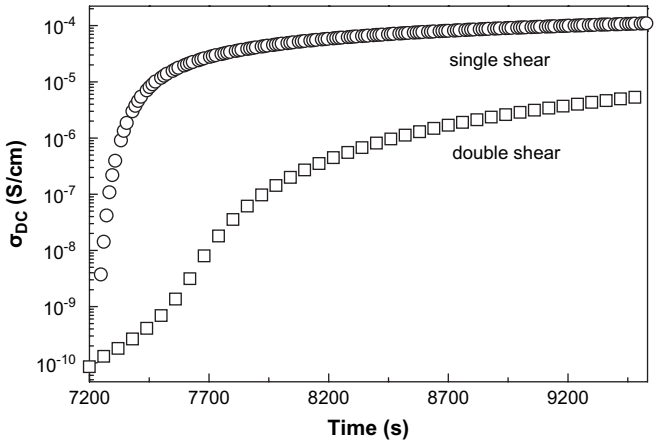

Fig. 4. Comparison of DC conductivity σ_{DC} recovery for single (a) and (b) double shear regimes. The data were taken from Fig. 3a and b.

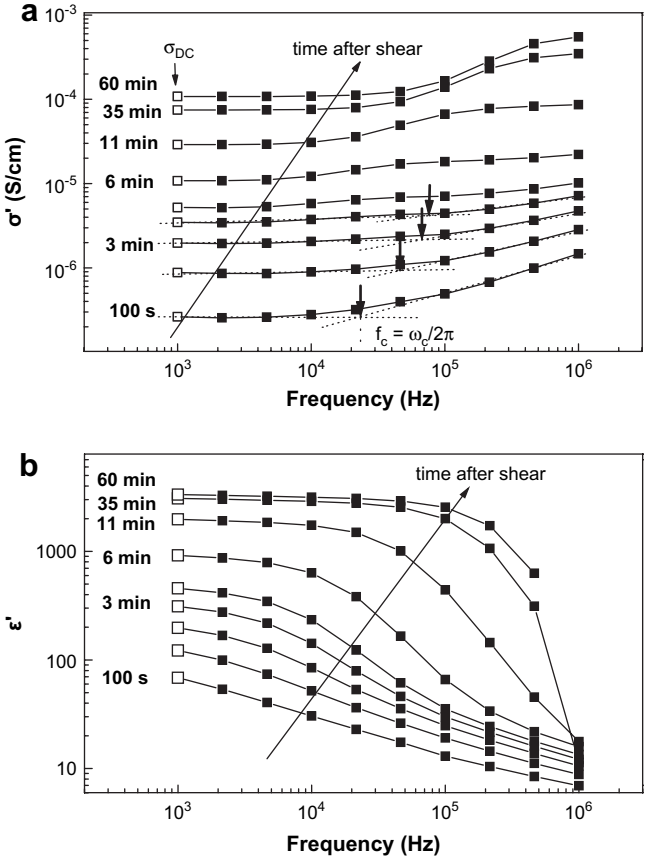

Fig. 5. Frequency dependence of the real part of complex electrical conductivity σ' (a) and the real part of permittivity ε' (b) after a short shear deformation (single shear experiment, see text). f_c is the cross-over frequency (see text).

In Fig. 5a, showing the real part of the complex conductivity σ' as a function of time (conductivity recovery time after single shear at 230 °C), short arrows indicate the cross-over frequencies f_c ($=\omega_c/2\pi$). Although the "slowing down" of f_c below the percolation threshold cannot be identified in our experiment, the increase of f_c for recovery times between 100 s and 6 min is indicating a system with increasing content of conductive sites (here increasing content of conductive agglomerates) for $p > p_c$. For longer recovery times ($t > 6$ min) a second process (step-like increase) dominates the conductivity spectra. We relate this process to a Maxwell–Wagner polarisation due to additional capacities appearing in the system. From the tremendous increase in the dielectric permittivity (Fig. 5b) in the same time interval, one can assume that the large number of small capacitors formed at the CNT–polymer–CNT contacts is responsible for this process. A similar process was found for carbon black in rubber and was related to capacitors formed by the bound rubber [32]. The increase of the low frequency permittivity (open symbols in Fig. 5b) deviates from the theoretically expected behaviour above percolation and was explained previously by the formation of microcapacitors in the contact region between CNTs [11].

3.2. Recovery of the shear modulus

The dynamic-mechanical properties of the composite melts after shear deformation were measured in parallel with the dielectric measurements in order to find a correlation between the recovery of the electrical conductivity and the mechanical properties. The real part G' of the complex shear modulus ($G^* = G' + iG'$) measured at $\omega = 1$ rad/s as a function of the rest time after shear is shown in Fig. 6 for the two shear regimes (single and double). The circles represent the modulus recovery after single shear deformation (10 rad in 10 s), whereas the squares represent the G' data after double shear deformation (short pre-shear of 10 rad in 1 s and second shear of 10 rad in $t = 10$ s, with 6 min of rest in-between).

The double sheared sample shows a slower recovery and lower value of the storage modulus G' than the sample sheared moderately (single shear). This trend is similar to the recovery kinetics of the DC conductivities (see Fig. 4) and can be also explained by different degrees of destruction of the CNT network. The shape of the two curves, however, is similar. In order to understand the modulus recovery, the dynamic mechanical spectra $G'(\omega)$ were measured for different recovery times in the oscillation frequency range from 0.3 to 100 rad/s with a small strain amplitude (see Section 2.3). Fig. 7 shows the time evolution of the G' spectra after single shear.

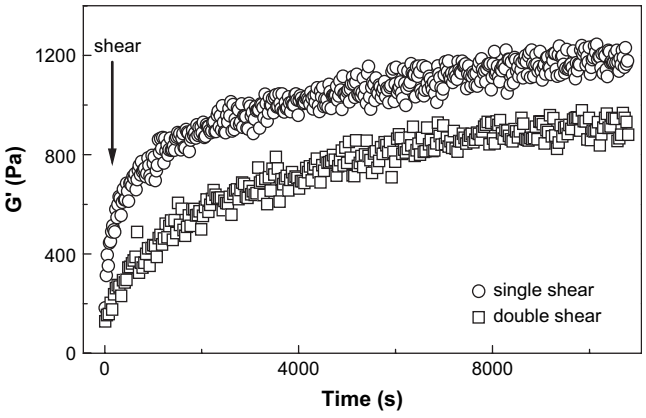

Fig. 6. Recovery of the storage modulus G' versus time for the single (circles) and double shear (squares) experiment. The experimental procedure is described in the text.

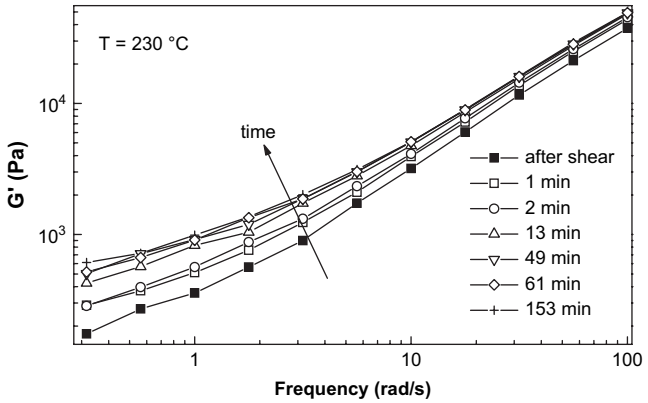

Fig. 7. Frequency dependence of the storage modulus G' as a function of rest time after a short shear deformation (single shear experiment).

For the explanation of the composition-dependent changes in rheological data of polymer–CNT composites a rheological percolation threshold is often assumed [33–35]. An alternative description of the changes of rheological properties induced by the formation of a filler network embedded in a viscoelastic liquid is the so-called "liquid–solid-like transition" [36]. Some time ago, we discussed the rheological data of a polymer melt filled with carbon nanotubes in terms of three types of network structures [13]: (i) the temporary polymer–polymer network formed by entanglements, (ii) the carbon nanotube network and (iii) the combined carbon nanotube–polymer network. A similar description was given in Ref. [35]. At moderate deformations no significant topological restraints between nanotubes are expected. Furthermore, the nanotubes in a polymer melt are assumed to be separated in their contact region by polymer chains and not really touch each other. Therefore, for small strain amplitudes the contribution of the geometrical CNT network (ii) to the rheological properties can be almost neglected. For this assumption the shear modulus can be described as a mixture of the modulus of the polymer matrix (entangled polymer chains) and that of the combined carbon nanotube–polymer network [13]. This assumption will be used in Section 3.4 for modelling of the data.

3.3. Modelling of conductivity recovery

In order to understand the recovery of the nanotube network after shear and the related conductivity behaviour in polymer melts a simple model was recently proposed [20] by combining two approaches: the classical percolation theory for conductive/insulating systems and a model for cluster aggregation. Since agglomerates were experimentally observed in the composites (Fig. 1c) such an approach seems to be reasonable. In order to keep the advantages of the percolation theory – which assumes a homogeneous distribution of conductive filler particles – and to describe the time dependent change of conductivity for a fixed CNT content, a time dependent agglomerate concentration was introduced. These agglomerates are assumed to be conductive objects formed by loosely packed nanotubes. At their contact areas the nanotubes (inside these agglomerates) are assumed to have distances in the nanometer range which allows electron tunnelling. This was also proposed for carbon black polymer composites by several authors (see Ref. [37] and references therein). The strong dependence on distance explains the different conductivities of agglomerates and of the matrix containing well dispersed nanotubes.

The formation of the agglomerates in a polymer matrix is a complex process at different length scales. The driving force is assumed to be a combination of strong dispersive interactions between filler particles and polymer chains and depletion interaction

between adjacent particles [37]. The latter is an attractive force of entropic origin which arises from the difference in free energy of the surrounding polymer matrix and the chains between two filler particles. The competition of both interactions (here: depletion and CNT–polymer interaction) leads to the characteristic gap (see also Section 3.1) at the filler particle contacts. In order to describe the agglomeration process we used a kinetic equation of second order ("collision of two particles"). We are aware that this is an oversimplification. For instance at late stages the growth of a network should follow rather first order kinetics. Alternatives would be a set of hierarchical equations or a spinodal decomposition into CNT-poor and CNT-rich phases. Furthermore, the destruction of the conductive network during shear is not yet considered.

The theory of the electrical percolation gives the following expression for the DC conductivity above the percolation threshold p_c as a function of filler concentration (for example, see Refs. [11,20,37] and references therein):

$$\sigma_{DC} = \sigma_{0A}\left(\frac{p_A - p_c}{1 - p_c}\right)^t, \quad p > p_c. \tag{2}$$

where p_A is the volume concentration of the conductive agglomerates contributing to the percolation network, $t = 2$ is an exponent usually taken for 3D system [38–44], and σ_{0A} is the conductivity of agglomerates formed by CNTs. The DC conductivity below the percolation threshold p_c as a function of agglomerate concentration is given by:

$$\sigma_{DC} = \sigma_{0M}\left(\frac{p_c - p_A}{p_c}\right)^{-s}, \quad p < p_c. \tag{3}$$

where σ_{0M} is the conductivity of the polymer matrix. For fitting the data a value of $s = 0.73$ has been taken from literature [39,45–47]. An alternative equation for the dependence of the electrical conductivity on conductive filler concentration was proposed by Fournier et al. [48] and was successfully applied to polymers containing CNT [49–51]. However, since this equation seems to be rather empirical we do not follow this route here.

The growth of the conductive network was considered as an agglomeration process in which two particles T, which do not contribute to the total conductivity, interact and create a conductive (spherical) agglomerate A. This leads to a time-dependent volume concentration $p_A(t)$ in Eqs. (2) and (3).

For formation of a (infinite) filler network in elastomers Heinrich et al. [25] proposed a second order kinetics. This idea is transferred here to the agglomeration process in polymer–CNT composites:

$$\frac{dN_A}{dt} = kN_T^2, \tag{4}$$

where N_T and N_A are the numbers of particles T and A, respectively, per unit volume (number density), and k is the reaction rate. For an agglomeration of two particles T the boundary condition $N_T(t) = N_{T0} - 2(N_A(t) - N_{A0})$ has to be fulfilled. N_{T0} and N_{A0} are the starting number densities of particles T and agglomerates A, respectively. By solving Eq. (4) together with the condition for $N_T(t)$ one obtains the number density of agglomerates A as a function of time:

$$N_A(t) = N_{A0} + \frac{N_{T0}}{2}\left(1 - \frac{1}{1 + 2ktN_{T0}}\right), \tag{5}$$

A similar equation can be written for the volume concentration of agglomerates A by rescaling the number densities $N_T(t)$ and $N_A(t)$ by the factors of V_T and V_A, which are the effective volumes occupied by a particle T and a spherical agglomerate A, respectively. Finally, the re-scaled Eq. (5) for volume concentrations is:

$$p_A(t) = p_{A0} + (p_{A\infty} - p_{A0})\left(1 - \frac{1}{1 + 4k't(p_{A\infty} - p_{A0})}\right), \tag{6}$$

with the modified reaction rate constant $k' = k/V_A$ and the final value ($t \to \infty$) for the volume concentration of the agglomerates $p_{A\infty}$. Assuming that finally all nanotubes belong to one of the agglomerates, the parameter $p_{A\infty}$ can be calculated as the ratio of the total volume concentration of nanotubes in the sample, p_{NT}, and the volume concentration of nanotubes inside an agglomerate, $p_{NT,Aggr}$: $p_{A\infty} = p_{NT}/p_{NT,Aggr}$. Eqs. (2) and (3), with p_A from Eq. (6), describe the electrical conductivity of a system with increasing volume concentration of agglomerates.

Fig. 8a shows the experimental DC conductivities versus time for the single and double shear experiments in a log–log scale together with the fitting curves for $p_A(t) < p_c$ (dashed line) and for $p_A(t) > p_c$ (solid line) using Eqs. (2), (3) and (6). In our fitting procedure all data for $p_A(t) < p_c$ and $p_A(t) > p_c$ as well as for both curves (single and double shear) were fitted simultaneously using a combined non-linear fitting procedure (*Altaxo*).

The fitting parameters for both single and double shear are presented in Table 1. Assuming that the agglomerates are spherical objects, the percolation threshold p_c was fixed to 20 vol%. The exponents s and t were fixed to values of 0.73 and 2, respectively (see

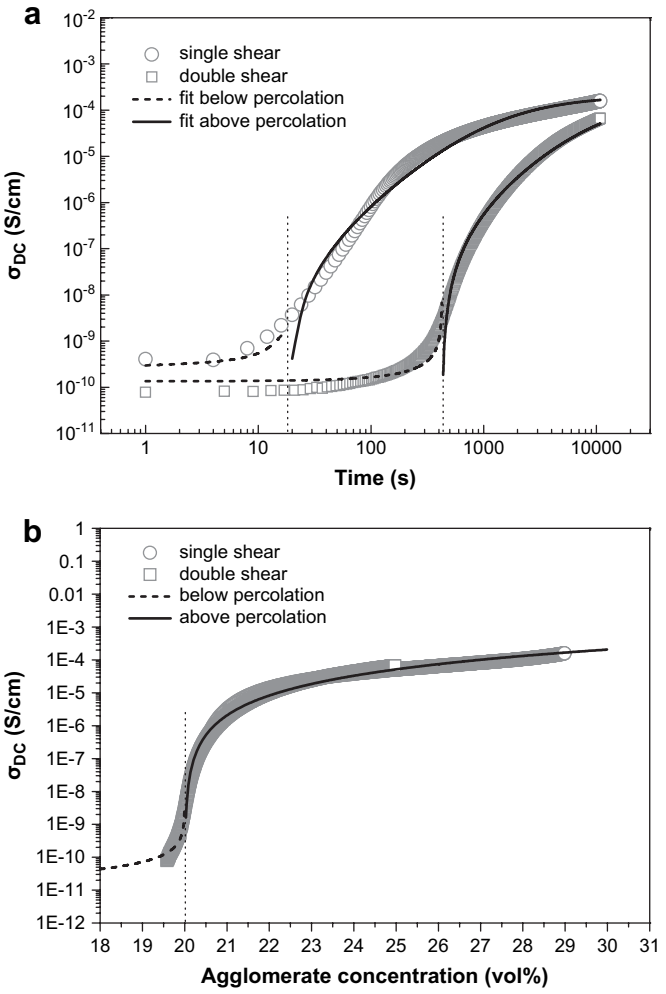

Fig 8. (a) Simultaneous fitting of the DC conductivities for single (circles) and double (squares) shear experiments with a combined cluster aggregation/percolation model (dashed and solid lines below and above percolation, respectively). (b) Experimental DC conductivities (from Fig. 8a) as a function of the calculated agglomerate concentration for single (circles) and double (squares) shear experiments. The percolation transitions are indicated by dotted lines. The fitting parameters are given in Table 1.

Table 1
Fitting parameters for the combined cluster aggregation/percolation model with fixed critical exponents ($s = 0.73$ and $t = 2$)

Experiment	$p_{A\infty}$ (vol%)	p_{A0} (vol%)	k' (s^{-1})	p_c^{eff} (vol%)	σ_{0M} (S/cm)	σ_{0A} (S/cm)
Single shear	(30)	19.85	$2.05\ 10^{-3}$	(20)	$8.13\ 10^{-12}$	$1.32\ 10^{-2}$
Double shear	(30)	19.58	$2.38\ 10^{-4}$	(20)	$8.13\ 10^{-12}$	$1.32\ 10^{-2}$

Single and double shear experiments were fitted together. The parentheses indicate that the parameters were fixed during the fitting procedure.

above). The volume content of the agglomerates for long recovery times was estimated from Fig. 1c (white circles) to be about 30 vol% and also set fixed in the fitting procedure. This results in a volume content of 2 vol% of nanotubes in the agglomerates and corresponds to an agglomerate conductivity of σ_{0A} of 10^{-2} S/cm [13], which is close to the value resulting from the fit. The p_{A0} and k' values are different for single and double shear. It should be noted that the quality of the fit is nearly independent of the actual choice of p_c and $p_{A\infty}$.

The agreement between the modelled curves and the experimental data (Fig. 8a) is satisfactory for both single and double shear experiments. Although the choice of the parameters includes some arbitrariness, this supports the idea of combination of a kinetic equation for filler agglomeration and electrical percolation. While assuming for both experiments the same nanotube packing density and the same conductivity of agglomerates, different values of k' were obtained from the fit. Since the matrix viscosity should be identical for both experiments this difference is surprising. However, different shear conditions may result in different spatial distribution of agglomerates which lead to different kinetics of the network formation process.

The DC conductivities (from Fig. 8a) are plotted in Fig. 8b as a function of the calculated agglomerate concentration $p_A(t)$. This plot looks similar to those commonly presented for the electrical percolation transition in DC conductivity as a function of filler content [11]. Here the concentration of conductive elements (agglomerates) changes not because they were added to the polymer matrix, but their concentration is increasing by an agglomeration process. The overlap of the experimental data in the "master plot" (Fig. 8b) supports the consistency of our simple model for different shear prehistory.

The quality of the fit (not shown) can be improved by setting the exponents s and t as free fit parameters. The corresponding values are given in Table 2 for single and double shear. It should be stated here that using the equation proposed by Fournier et al. [48] the data could be also fitted with sufficient quality.

3.4. Modelling of rheological recovery

In the following section we make an attempt to extend the cluster aggregation idea to the recovery of the shear modulus. From the comparison of Figs. 3 and 6 it is obvious that the DC conductivity changes by several orders of magnitude, whereas G' increases only over one order of magnitude. At a first glance this discrepancy can be explained by different mechanisms: (i) charge carrier transport for electrical conductivity and (ii) mechanical momentum transfer for rheological properties. The first mechanism needs close electrical contacts of about 10 nm (for hopping or tunnelling) [52] between the conductive network parts, while the second mechanism needs a viscous coupling between tubes, agglomerates and polymer chains. Here we try to model the mechanical properties by "solid-like" filler particles in a polymer matrix. The "filler particles" are assumed to be identical to the conductive agglomerates and to follow the same kinetics. The idea to model the modulus recovery after shear by formation of contacts between filler particles was proposed by Heinrich et al. [25] for elastomers and polyethylene with fillers. However, it was not possible here to fit the data in Fig. 6 by a linear dependence between the number density of agglomerates (given by Eq. (5)) and the modulus increase. Therefore, we tested different mixing laws (see references in Ref. [53]) for the polymer–agglomerate composite.

The upper and lower bounds, restricting the dependence of the modulus G^* on the volume fraction of the filler, are given by a "parallel" model (Voigt) as:

$$G^* = (1-\phi_A)G_P^* + \phi_A G_A^*, \tag{7}$$

and by a "series" model as:

$$1/G^* = (1-\phi_A)/G_P^* + \phi_A/G_A^*, \tag{8}$$

where ϕ_A ($\equiv p_A$) is the volume fraction of the agglomerates. G_A^* is the shear modulus of the agglomerates and G_P^* is the modulus of the polymer phase. At 230 °C, G_A^* and G_P^* were taken to be 3300 and 50 Pa, respectively. G_A^* was extrapolated from the rheological data in Ref. [33] at 1 rad/s and 260 °C for CNT content of about 2.5 wt%. The CNT concentration inside an agglomerate was taken as constant.

For spherical particles included in a matrix the Kerner model [54] can be applied. According to this model the modulus of the composite is given by:

$$G^* = G_A^* \frac{\phi_P G_P^* + (\gamma+\phi_A)G_A^*}{(1+\gamma\phi_A)G_P^* + \gamma\phi_P G_A^*}, \tag{9}$$

where $\gamma = 2(4-5\nu)/(7-5\nu)$ and $\nu = 0.37$ is Poisson's ratio of the composite. A model which predicts phase inversion at intermediate compositions was developed by Budiansky [55]:

$$\frac{\phi_P}{1-\varepsilon\left(\frac{G_P^*}{G^*}-1\right)} + \frac{\phi_A}{1-\varepsilon\left(\frac{G_A^*}{G^*}-1\right)} = 1, \tag{10}$$

where $\varepsilon = 2(4-5\nu)/15(1-\nu)$.

As mentioned above, the properties of a two-phase composite of any geometry will lie between the parallel and the series models. Kerner model is close to the series model, whereas the Budiansky model yields a drastic change (phase inversion) in the mixing law over a small ϕ_A range.

The curves for the real part of the shear modulus calculated by different mixing models (Eqs. (7)–(10)) are plotted in Fig. 9 together with the experimental shear modulus G' (from Fig. 6). The time axis in Fig. 6 is re-scaled by the concentration of agglomerates p_A ($\equiv\phi_A$) using Eq. (6) with the parameters given in Table 1.

It can be clearly seen that none of the models yields a satisfactory approximation of the experimental data. However, there

Table 2
Fitting parameters for the combined cluster aggregation/percolation model with free exponents s and t

Experiment	$p_{A\infty}$ (vol%)	p_{A0} (vol%)	k' (s^{-1})	p_c^{eff} (vol%)	s	t	σ_{0M} (S/cm)	σ_{0A} (S/cm)
Single shear	(30)	19.53	7.00×10^{-3}	(20)	1.32	3.04	2.33×10^{-12}	7.30×10^{-2}
Double shear	(30)	18.73	7.27×10^{-4}	(20)	1.32	3.04	2.33×10^{-12}	7.30×10^{-2}

Single and double shear experiments were fitted together. The values in parentheses were fixed during the fitting procedure.

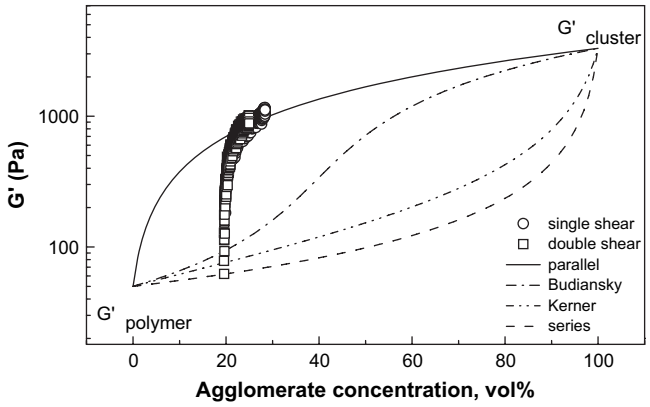

Fig. 9. Real part of the shear modulus G' for single (circles) and double shear (squares) experiments plotted versus calculated agglomerate concentration. The lines represent different mixing laws (see legend). The details are described in the text.

seems to be a transition from the series to the parallel model at about 20 vol% of agglomerates. This may indicate a transition from a rheological behaviour dominated by the polymer matrix to a behaviour dominated by the filler network.

4. Summary and conclusions

In this paper a combined investigation of the electrical and rheological properties of PC–MWNT melts was performed using simultaneous dielectric and mechanical measurements during annealing of the as-received samples and in the rest time after different shear deformations. The shear deformation applied to the annealed composites containing 0.6 vol% MWNT leads to a tremendous decrease in the DC conductivity by 6 orders of magnitude as well as modulus decrease by a factor of 20 (i.e. down to the values of the polymer matrix). The decreases in the electrical conductivity and G' are explained by a destruction of the filler network. The following recovery of both electrical and mechanical properties is attributed to the re-formation of the network of interconnected nanotube agglomerates. The agglomeration of nanotubes was assumed to be a key process defining physical properties of polymer/MWNT melts.

The reformation of the conductive network was described by a combination of cluster aggregation and percolation theory. Within this model, the electrical conductivity recovery was explained as a dynamic percolation of conductive nanotube agglomerates of spherical shape. Following this assumption, the conductivity recovery curves for different shear prehistory could be reduced to one "master curve" by replacing the time axis by the calculated agglomerate concentration. The idea of cluster aggregation was applied to the recovery of the shear modulus as well. The agglomerates are assumed to act here as "solid-like" filler particles in the polymer matrix. Different mechanical mixing laws were tested: series, parallel, Kerner and Budiansky models. However, none of these models yields a satisfactory approximation of the rheological data.

In conclusion, combined rheological and conductivity measurements provide new experimental information for better understanding of the agglomeration kinetics in polymer melts containing carbon nanotubes. The methodological approach can be extended to other nanofillers in polymers as well. For more quantitative understanding of the influence of mechanical deformations on the electrical and rheological properties it is also necessary to investigate the network destruction in detail. Furthermore, the proposed cluster aggregation kinetics together with the dynamic percolation picture, and the mechanical mixing laws are only first attempts to describe the time dependence of electrical and rheological properties. An alternative to cluster aggregation would be a spinodal decomposition into a CNT-rich and a CNT-poor phase. Those alternative models should be tested in future.

Acknowledgments

This project was funded by the Bundesministerium für Wirtschaft und Arbeit via the Arbeitsgemeinschaft industrieller Forschungsgesellschaften (AiF Projects Nos. 122 ZBG and 144454N). We would like to thank Sven Pegel (IPF Dresden) for sample preparation and Wolfgang Böhm (DKI) for performing the combined DRS-DMA experiments. Furthermore, we thank Martin Engel (DKI and TU Darmstadt) for pre-experiments and for his contribution to the model. IA would like to thank Gert Heinrich for his hints and helpful discussions on cluster aggregation kinetics and filler networks. The authors would like to thank Hyperion Catalysis Inc. for providing materials.

References

[1] Klüppel M, Schuster RH, Heinrich G. Rubber Chem Technol 1997;70:243.
[2] Klüppel M. Adv Polym Sci 2003;164:1–86.
[3] Klüppel M, Heinrich G. Rubber Chem Technol 1995;68:623.
[4] Thostenson ET, Li C, Chou TW. Compos Sci Technol 2005;65:491–516.
[5] Breuer O, Sundararaj U. Polym Compos 2004;25(6):630–45.
[6] Coleman JN, Khan U, Gun'ko YK. Adv Mater 2006;18(6):689–706.
[7] Sandler JKW, Kirk JE, Kinloch IA, Shaffer MSP, Windle AH. Polymer 2003;44(19):5893–9.
[8] Jiang X, Bin Y, Matsuo M. Polymer 2005;46:7418–24.
[9] Andrews R, Jacques D, Minot M, Rantell T. Macromol Mater Eng 2002;287:395–403.
[10] Coleman JN, Cadek M, Blake R, Nicolosi V, Ryan KP, Belton C, et al. Adv Funct Mater 2004;14:791–8.
[11] Pötschke P, Dudkin SM, Alig I. Polymer 2003;44:5023–30.
[12] Pötschke P, Bhattacharyya AR, Alig I, Dudkin SM, Leonhardt A. AIP Conf Proc 2004;723:478–82.
[13] Pötschke P, Abdel-Goad M, Alig I, Dudkin S, Lellinger D. Polymer 2004;45:8863–70.
[14] Pötschke P, Bhattacharyya AR, Alig I, Dudkin SM, Leonhardt A. AIP Conf Proc 2005;786:595–601.
[15] Anand AK, Agrawal US, Joseph R. J Appl Polym Sci 2007;104:3090–5.
[16] Alig I, Pötschke P, Pegel S, Dudkin SM, Lellinger D. Gummi Fasern Kunstst 2007;60:280–3;
Rubber Fibres Plast Int 2008;3(2):92–5.
[17] Alig I, Lellinger D, Dudkin S, Pötschke P. Polymer 2007;48:1020–9.
[18] Alig I, Lellinger D, Engel M, Skipa T, Pötschke P. Polymer 2008;49:1902–9.
[19] Zhang C, Wang P, Ma C, Wu G, Sumita M. Polymer 2006;47:466–73.
[20] Alig I, Skipa T, Engel M, Lellinger D, Pegel S, Pötschke P. Phys Status Solidi B 2007;244:4223–6.
[21] Kharchenko SB, Douglas JF, Obrzut J, Grulke E, Migler KB. Nat Mater 2004;3:5648.
[22] Obrzut J, Douglas JF, Kharchenko SB, Migler KB. Phys Rev B 2007;76:195420.
[23] Hobbie EK, Wang H, Kim H, Lin-Gibson S, Grulke EA. Phys Fluids 2003;15(5):1196–202.
[24] Hobbie EK, Fry DJ. J Chem Phys 2007;126:124907.
[25] Heinrich G, Costa FR, Abdel-Goad M, Wagenknecht U, Lauke B, Härtel V, et al. Kautsch Gummi Kunstst 2005;58(4):163–7.
[26] Schüler R, Petermann J, Schulte K, Wentzel HP. Macromol Symp 1996;104:261–8.
[27] Schüler R, Petermann J, Schulte K, Wentzel HP. J App Polym Sci 1997;63:1741–6.
[28] Pegel S, Pötschke P, Petzold G, Alig I, Dudkin SM, Lellinger D. Polymer 2008;49:974–84.
[29] Balberg I. Philos Mag B 1987;56:991–1003.
[30] Heermann DW, Stauffer D. Z Phys B 1981;44:339.
[31] Ziff RM, Stell G. LaSC, University of Michigan, Report no. 88–4, Footnote 26;1988.
[32] Kastner A. Ph.D. thesis, TU-Darmstadt; 2001.
[33] Pötschke P, Fornes TD, Paul DR. Polymer 2002;43:3247–55.
[34] Meincke O, Kaempfer D, Weickmann W, Friedrich C, Vathauer M, Warth H. Polymer 2004;45:739–48.
[35] Du F, Scogna RC, Zhou W, Brand S, Fischer JE, Winey KI. Macromolecules 2004;37:9048–55.
[36] Winter HH, Mours M. Adv Polym Sci 1997;134:165–234.
[37] Meier JG, Mani JW, Klüppel M. Phys Rev B 2007;75:054202.
[38] Bunde A, Havlin S. In: Bunde A, Havlin S, editors. Fractals and disordered systems. Berlin, Heidelberg, New York: Springer; 1996.
[39] Sahimi M. Applications of percolation theory. London: Taylor & Francis Ltd.; 1994.

[40] Fish R, Harris AB. Phys Rev B 1978;18(1):416–20.
[41] Adler J, Meir Y, Aharony A, Harris AB, Klein L. J Stat Phys 1990;58:511.
[42] Adler J. J Phys A Math Gen 1985;18:307–14.
[43] Alexander S, Orbach R. J Phys Lett (Paris) 1982;43:L625.
[44] Gingold DB, Lobb CJ. Phys Rev B 1990;42(13):8220–4.
[45] Clerc JP, Giraud G, Laugier JM, Luck JM. Adv Phys 1990;39(3):191–309.
[46] Stauffer D, Aharony A. Introduction to percolation theory. London: Taylor & Francis Ltd.; 1994.
[47] Herrmann HJ, Derrida B, Vannimenus J. Phys Rev B 1984;30(7):4080–2.
[48] Fournier J, Boiteux G, Setre G, Marchy G. Synth Met 1997;84:839–40.
[49] Coleman JN, Curran S, Dalton AB, Davey AP, McCarthy B, Blau W, et al. Phys Rev B 1998;58:7492–5.
[50] Curran SA, Zhang D, Wondmagegn WT, Ellis AV, Cech J, Roth S, et al. J Mater Res 2006;21:1071–7.
[51] McCullen SD, Stevens DR, Roberts WA, Ojha SS, Clarke LI, Gorga RE. Macromolecules 2007;40:997–1003.
[52] Ruschau GR, Yoshikawa S, Newnham RE. J Appl Phys 1992;72:953–9.
[53] Alig I, Tadjbakhsch S, Floudas G, Tsitsilianis C. Macromolecules 1998;31:6917–25.
[54] Kerner EH. Proc Phys Soc London 1956;B69:809.
[55] Budiansky B. J Mech Phys Solids 1965;13:223.